Institute of Physics Publishing Journal of Physics: Conference Series **50** (2006) 50–61
doi:10.1088/1742-6596/50/1/006 5th International Conference on Physics and Astrophysics of Quark Gluon Plasma

Photon measurements in forward rapidity in heavy-ion collisions

Yogendra Pathak Viyogi
Variable Energy Cyclotron Centre, 1/AF, Bidhan Nagar, Kolkata 700064
E-mail: viyogi@veccal.ernet.in

Abstract.
Contribution of a preshower photon multiplicity detector to the physics of ultra-relativistic nuclear collisions is reviewed and future possibilities at RHIC and LHC are discussed.

.

1. Introduction

One of the main goals of the high energy heavy-ion collision program is to look for the possible formation of Quark-Gluon Plasma (QGP). In the collision process the system may go through a phase transition from confined hadronic matter to a deconfined state of quarks and gluons which will be a transient state. The system then evolves from a very hot and dense QGP state to normal hadronic matter by undergoing cooling, expansion and hadronization. Information obtained from various global observables (e.g photon multiplicity (N_γ), charged particle multiplicity (N_{ch}) and transverse energy) is used to characterize the system formed in such collisions. Study of photon production has shown a great promise in studying the various aspects of the reaction mechanism in such collisions and dynamics of particle production [1, 2, 3, 4, 5, 6, 7, 8, 9, 10].

The measurement of photons in high energy physics experiments has been traditionally carried out using calorimeters. Due to large spatial density of produced particles in the forward rapidity region in ultra-relativistic nuclear collisions, and consequent overlap of showers, one cannot use calorimeters beyond a certain region. In such a situation, a limited goal of photon study can be achieved using a preshower detector having a relatively thinner converter and restricting the development of shower. The preshower detector can only measure the spatial distribution of photons but not their energies.

Such a preshower photon multiplicity detector (PMD) has been employed in SPS and RHIC experiments and is planned also for the LHC experiment. In addition to extending the phase space coverage for the measurement of pseudorapidity distributions, the PMD data on spatial distribution of photons, along with other measurement of charged particle multiplicity and event centrality, has been able to address the following important physics topics related to phase transition and chiral symmetry restoration:

- determination of the reaction plane and the probes of thermalization via studies of azimuthal anisotropy and flow;
- critical phenomena near the phase boundary leading to fluctuations in global observables like multiplicity and pseudorapidity distributions;

- signals of chiral-symmetry restoration (e.g. disoriented chiral condensates) through the measurement of charged-particle multiplicity ($N_{\rm ch}$) also in a common part of phase space and study of the observables $N_\gamma/N_{\rm ch}$ with full azimuthal coverage.

2. Photon Multiplicity Detector

The preshower detector for measuring photon multiplicity consists of a thin converter behind which is placed an array of sensitive detection elements (cells or pads). The thickness of the converter is chosen such that it provides a reasonably large signal for electromagnetic particles, restricts shower size to a few cells and the response to charged hadrons is limited to preferably one pad or cell. The thickness of the converter and the granularity (size, shape of one detection element) have to be optimized using Monte-Carlo simulations. A second plane of similar granularity may be placed in front of the converter for improving the discrimination between charged hadrons and photons.

2.1. Detector for the SPS experiments

The PMD for the fixed target SPS experiments was made using plastic scintillator pads, with scintillation light being transported to readout devices using wavelength shifting fibers. The light at the fibre ends were converted to electrical signals and readout using the image intensifier (II) and CCD camera systems obtained from the old UA2 experiment at CERN. The basic parameters of the two detectors, used in the WA93 and WA98 experiments, are summarized in Table 1. These had only one plane of detection elements behind a 3 X_0 thick lead converter.

2.1.1. PMD for the WA93 experiment : The first PMD, made for the WA93 experiment, consisted of 7500 plastic scintillator pads and had long WLS fibers for transporting scintillation light to the II+CCD camera readout system [11]. The pads were square in shape and having uniform size of 2 cm. These were placed in four quadrants of a light-tight box, each quadrant having 1875 pads arranged in a matrix of 50 $\times$ 38 with a space for 5 $\times$ 5 pads left for the hole of the beam pipe. The fiber bundle from each quadrant was read out using one camera system.

The detector, mounted at 10.5m from the target, covered the pseudorapidity region $2.8 \leq \eta \leq 5.2$ of which the region $3.3 \leq \eta \leq 4.9$ had full azimuthal coverage. It was installed in 1991 and was used to study the collisions of 200 A.GeV sulphur ions with gold nuclei during 1991 and 1992 SPS run periods.

2.1.2. PMD for the WA98 Experiment : The PMD for the WA98 experiment was also based on the plastic scintillator pads, with light being transported using WLS fibres [12]. Based on the experience gained during the operation of the WA93 PMD, the fabrication technology was modified for improvements in light collection and reduction of the distortion of the image at the CCD. The WLS fibres of short length were coupled to long lengths of clear fibres to reduce light attenuation and a black paint was used in bundling the fibre ends to reduce spreading of the image on the CCD. To make the hit density nearly uniform over the detector, four different pad sizes, ranging from 15mm square to 25 mm square, were used, inner part having smaller pads and outer parts having larger pads. The detector consisted of 28 individual light-tight box modules, each having a matrix of 50$\times$38 scintillator pads read out using one image intensifier and CCD camera system.

The detector extended to an area of 21 sq.m. It was installed at 21.5 m from the target and covered the pseudo-rapidity region $2.5 \leq \eta \leq 4.2$, of which the region η= 3.2-4.0 had full azimuthal coverage. It is shown in Fig. 1. It was installed in the experiment in 1994 and took data for lead ion induced collisions at 158.A GeV energy during 1994 to 1996 SPS run periods.

Table 1. Parameters of WA93 and WA98 PMDs

Parameter	WA93	WA98
(η, ϕ) coverage	2.8-5.2 (2π in 3.3-4.9)	2.9-4.2 (2π in 3.2-4.0)
Number of readout cameras	4	28
Number of pads	7500	53200
Distance from target	10.5 m	21.5 m
Pad sizes (square shape)	20 mm	15 mm, 20 mm, 23 mm, 25 mm
Pad thickness	3 mm	3 mm
Light transport	WLS fibres	WLS + Clear fibres

2.2. Detector for colliders

For the next generation collider experiments at RHIC and LHC, it was soon realized that the PMD would have be made with a different technology. Scintillator pads with fibres were bulky and the readout systems were quite expensive. The collider environment required sleek detectors which could fit in a small space. It was also realized that with the increased multiplicity of produced particles, the detector design criteria had to be redefined, in particular charged particle hits on the preshower plane had to confined to a single pad or cell. Due to the presence of substantial number of electrons, the use of second plane in front of the converter also became necessary.

Using gas detectors, low cost readout could be obtained in the form of signal processing ASICs. However, existing gas detector technologies did not provide the solution to the containment of charged particle hits to a single detection unit.

An extensive R&D effort resulted in the design of a cellular honeycomb proportional counter, using Ar(70%)+CO_2(30%) as the sensitive medium and with novel ideas of extended cathode which provided almost uniform response to charged particles within the detector volume. This design offered all the advantages of lower cost and ease of construction for large area and highly granular detector system. The results of such an R&D are summarized in Ref. [13, 14].

The basic parameters of the PMD for the RHIC and LHC experiments are given in Table 2. In these detectors also we used 3 X_0 thick lead converter.

2.2.1. PMD for the STAR experiment at RHIC : The STAR PMD [15] consists of a set of super-modules arranged in two vertical halves so that each half moves independently around the beam pipe. The super-modules are of various shapes but all are made up of rhombus unit modules having 24×24 cells. The number of unit modules in the supermodules vary from 4 to 9. There are two planes of the sensitive detectors, one in front of the converter (acting as charged particle veto) and one behind the converter which registers preshower signals. There are 12 supermodules in each plane of the detector.

The signal processing for STAR PMD is done using GASSIPLEX chips, which has 16 channels of preamplifier and shaper and provides analog multiplexed output. One front-end electronics (FEE)-Board has 4 chips and is connected to a group of 64 cells in a 8×8 matrix on the detector. The digitization and readout of the analog multiplexed signals is done using C-RAMS modules. The track and hold flag is generated using a pre-trigger signal based on beam-beam counter in STAR because the actual Level 0 signal arrives rather late. Each block of C-RAMS handles signals from a chain of 27 FEE boards, i.e., for 1728 cells. There are in all 48 chains read out using 24 C-RAMS modules.

The detector is mounted in the STAR experiment at 540cm from the center of the TPC and

nominally covers the pseudorapidity region 2.3-3.8 with full azimuthal acceptance.

Fully instrumented preshower plane of the STAR PMD is shown in Fig. 2 in the data taking mode when the two halves are touching each other.

2.2.2. PMD for the ALICE experiment at the LHC : The PMD for the ALICE experiment consists of hexagonal cells having 0.23 cm^2 cross-section and 5 mm depth. Although originally proposed to use the cells identical to those used in the STAR PMD, the detector geometry was modified later due to constraints of available space within the ALICE experiment [16, 17].

The detector consists of rectangular shaped unit modules having 4608 cells. These unit modules are placed in supermdules which are separate gas-tight enclosures. There are two types of unit modules and super-modules, the difference being in the number of cells in the row and column, in one there are 48 rows and 96 columns while in the other there are 96 rows and 48 columns. There are 4 supermodules in each plane, arranged in such a way that each forms one quadrant of the detector. The detector can be opened as two halves around the beam pipe.

The design of signal processing electronics for the PMD is based on that of the tracking chambers of dimuon spectrometer in ALICE. The signals from the cells are processed using MANAS chips which provide analog multiplxed output for 16 channels. The readout of the analog multiplexed signals is performed, after digitization, using another custom built chip MARC and the CROCUS system.

The PMD will be mounted at 360cm from the center of the TPC in ALICE and will nominally cover the pseudorapidity region 2.3-3.5 with full azimuthal acceptance.

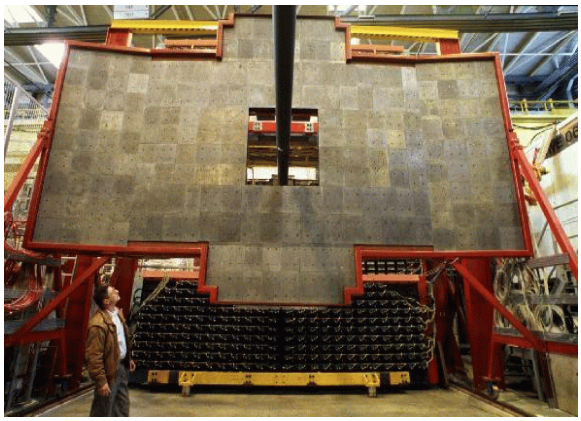

Figure 1. View of the WA98 PMD from the converter side. The sections on four sides were suitably inclined to provide near-normal incidence to incoming particles.

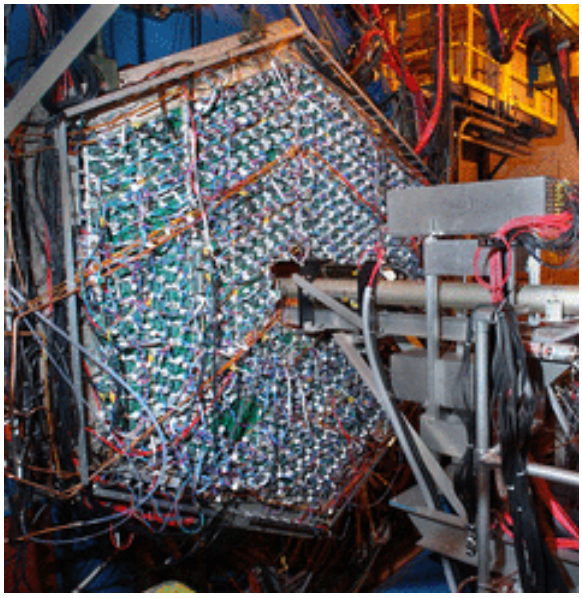

Figure 2. View of the preshower plane of STAR PMD from the RHIC tunnel side.

2.3. Photon reconstruction

The photon reconstruction is achieved by clustering the hits and then applying suitable algorithm to reject charged hadron hits. For the WA93/WA98 PMDs, where only the preshower plane of the detector was used, a simple algorithm based on a threshold on the cluster signal was used for the discrimination [5]. A more detailed algorithm based on neural network technique has

Table 2. Parameters of STAR and ALICE PMDs

Parameter	STAR@RHIC	ALICE@LHC
(η, ϕ) coverage	2.3-3.8, 2π	2.3-3.5, 2π
Number of planes	Preshower, veto	preshower, veto
Number of super-modules	24	8
Number of unit modules	144	48
Number of cells	83K	220K
Distance from vertex	540 cm	360 cm
Cell cross-section	1 cm^2	0.23 cm^2
Cell depth	8 mm	5 mm

also been investigated for PMD with charged particle veto [18] and used in the study of physics performance of ALICE PMD [13].

Due to interactions of charged hadrons in lead converter and the nature of the discrimination algorithm, the set of clusters finally labeled as 'photons' have some contaminants. The efficiency of photon reconstruction is usually around 70% and the purity of the photons in the accepted sample is also around 70%. These numbers vary with the system, centrality and pseudorapidity as studied using event generators and Monte-Carlo methods.

3. Physics results

The measurement of photon distributions in the forward rapidity region has made significant contributions to the physics at the SPS energy. The lower p_T cutoff for the PMD is only about 30 MeV/c [3, 13], thus enabling it to detect a large fraction of the photon spectrum. The presence of a charged particle multiplicity detector (SPMD) overlapping in phase space with the PMD has helped to greatly enhance the scope of physics studies using the PMD.

3.1. Pseudorapidity and multiplicity distributions

Pseudorapidity distribution of photons has been measured at various centralities using the PMD in WA93 experiment for S+Au collisions at 200.A GeV [3]. In general the shape of the distribution is well reproduced by the event generators like VENUS [19] but the absolute magnitude is somewhat underpredicted. Using the measurement of photon multiplicity by the PMD and the transverse e.m. energy by the MIRAC calorimeter, it was possible to study the centrality dependence of $< p_T >$ of photons [2].

The WA98 PMD measured photon production for Pb+Pb, Pb+Nb and Pb+Ni systems at 158.A GeV projectile energy. A systematic study of these data showed that VENUS again underpredicts the magnitude of pseudorapidity distributions [5]. Fig. 3 shows the minimum bias inclusive photon cross-section for the three systems along with the predictions of VENUS event generator with default parameters. The shape of these distributions is governed by the collision geometry. For asymmetric collisions of Nb and Ni targets small shoulders are present around N_γ of 300 and 200 respectively. This shoulder is produced when a decrease in the impact parameter leads to little increase in particle production and the cross-sections for these small impact parameter collisions pile up at a fixed N_γ.

The pseudorapidity distributions for the three systems studied are shown in Fig. 4 for various centralities. For the symmetric Pb+Pb collisions filled symbols represent the measured data and open symbols are reflections around η_{cm} (=2.92). The histograms show VENUS predictions. The discrepancy between data and VENUS is ∼10% for central collisions around mid-rapidity and

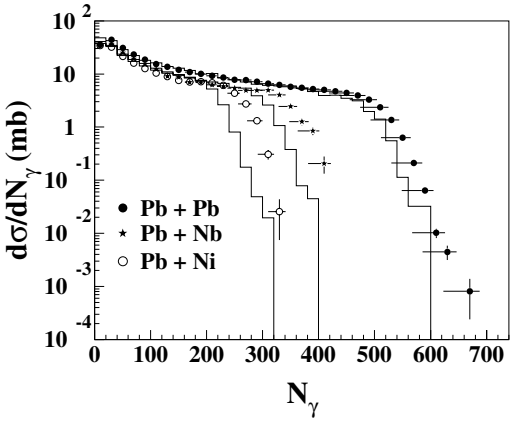

Figure 3. Minimum bias inclusive photon cross sections for Pb+Ni, Pb+Nb, and Pb+Pb reactions at 158·AGeV. Solid histograms are the corresponding distributions obtained from the VENUS event generator.

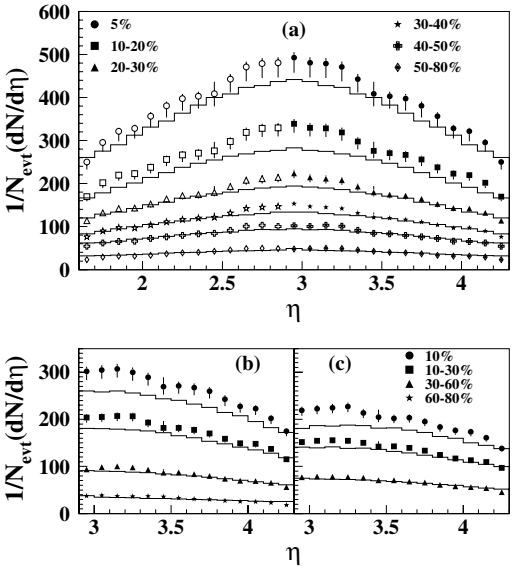

Figure 4. Pseudo-rapidity distributions of photons at various centralities in Pb induced reactions at 158·AGeV on (a) Pb, (b) Nb and (c) Ni targets. The solid histograms are the corresponding distributions obtained from the VENUS event generator.

decreases at larger impact parameters. For asymmetric systems the discrepancy between data and VENUS is comparatively larger.

An important observation of these systematic studies of photon production over a wide range of collision systems and centralities has been the scaling relation for total number of photons. It is found that this scales as a power law dependence on the number of participants, N_{part}, the exponent being 1.12±0.03 [5].

First results on photon distribution in the forward region at 62.4 GeV energy recently became available with the PMD in the STAR experiment [10]. These are described in detail in the article by B. Mohanty et al. in these proceedings [20]. At RHIC the HIJING model underpredicts photon production as measured by the PMD. However the AMPT model compares favorably well.

In Fig. 5 we have plotted the photon pseudorapidity distribution per participant nucleon in Au+Au collisions at 62.4A GeV as a function of η-y_{beam} for central collisions. Also superposed are the data from the WA98 experiment for the Pb+Pb collisions at 17.A GeV c.m. energy, from the WA93 experiment for S+Au collisions at 20.A GeV c.m. energy and from the UA5 experiment for *pp* collisions at 546 GeV. The data at SPS and at RHIC are found to be consistent with each other, suggesting that photon production follows limiting fragmentation behaviour. It is further found that the data are consistent with centrality- and energy- independent beahaviour similar to the results for identified charged particles [20].

3.2. Azimuthal anisotropy and flow

In the search for evidence of the phase transition from hadronic matter to quark gluon plasma in relativistic heavy-ion collisions, it is important to establish that thermalization occurs in the

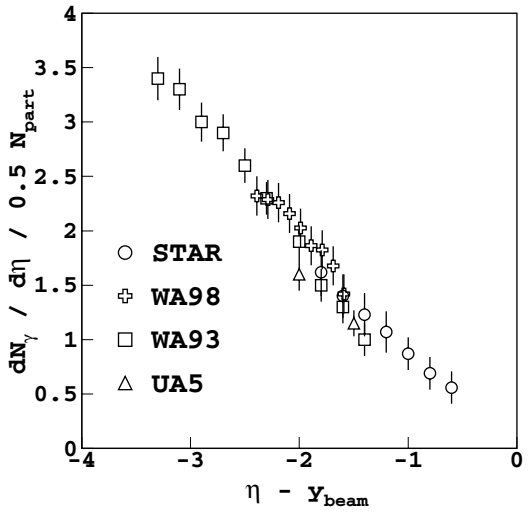

Figure 5. Limiting fragmentation as seen in the photon production.

reacting system. In non-central collisions the overlap volume, when projected onto the transverse plane, is not azimuthally symmetric. It has a smaller size along the direction of impact parameter than in the perpendicular direction. If thermal equilibrium is reached, collective flow develops with a velocity proportional to the pressure gradient, which is larger along the direction of impact parameter than along the perpendicular direction. Matter is thus expected to flow preferentially in the reaction plane which should result in an azimuthal anisotropy of the distribution of particles. In head-on collisions the anisotropy should disappear, even if thermalization occurs, due to the azimuthal symmetry of the overlap volume. Thus the study of anisotropy as a function of centrality assumes significance in the study of phase transitions.

The first observation of collective flow at the SPS energy came from the PMD data [1]. The anisotropy parameter[1] $\overline{\alpha}$ is plotted in Fig. 6 for the four centrality bins for the data (filled circles) and for the simulated data (open circles). The vertical bars indicate statistical errors only. The horizontal bars indicate the rms multiplicity of the bin. The estimated systematic errors are indicated by the bracket on each data point. The simulated events from VENUS event generator show a small anisotropy similar in magnitude to the estimated systematic error. The non-zero values are essentially due to π^0 decay correlations and finite multiplicity effects.

The extracted true anisotropies in the data are small but significantly greater than the simulation which does not include flow effects. The observed anisotropy decreases with decreasing impact parameter from $\overline{\alpha} \approx 0.07$ for peripheral collisions to $\overline{\alpha} \approx 0.045$ for central collisions. This dependence is similar, but the values are roughly half as large, as has been predicted by hydrodynamical model calculations [21].

The effect of photon correlation due to π^0 decay and other detector related effects on the deduced anisotropy values from photon measurements have been investigated in detail [22]. It has been shown that the measured anisotropy in photons can be used to deduce the anisotropy in parent neutral pions and a scaling relation between these two has been extracted in terms of an experimentally measurable quantity.

This concept has been tested and established in the analysis of data from the WA98 experiment [9]. For the study of anisotropy using data from the WA98 PMD, all the decay and detector effects were considered within a Monte-Carlo framework using the measured flow

[1] At that time the nomenclature of various flow coefficients were not standardized. In Ref. [1] the word 'directed flow' has been used for what is now commonly understood as elliptic flow and the notation $\overline{\alpha}$ is actually v_2.

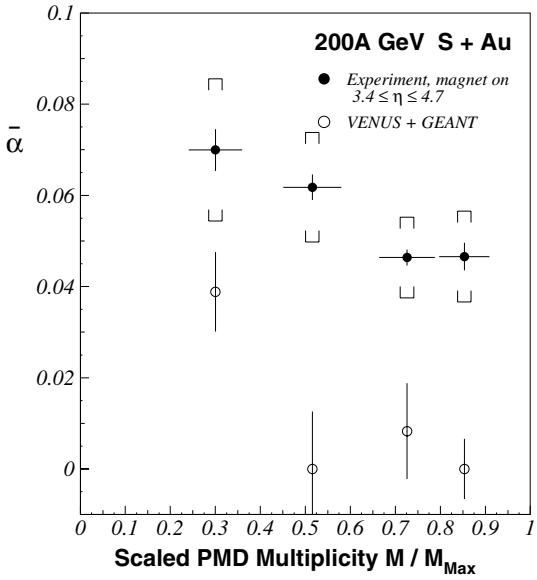

Figure 6. The true anisotropy $\bar{\alpha}$ as a function of the centrality (scaled multiplicity) for the experimental data (filled circles) and VENUS + GEANT simulations (open circles).

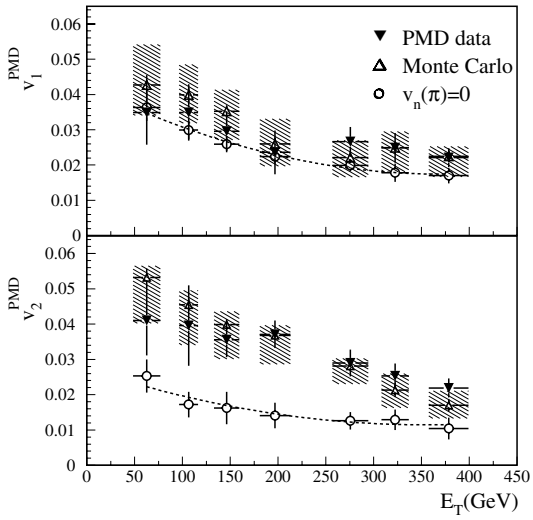

Figure 7. First order, v_1, and second order, v_2, anisotropy coefficients of the azimuthal distributions of photon hits for different centralities characterized by the measured transverse energy. The boxes indicate the extent of the estimated systematic errors.

values of charged particles in the same experiment within an overlapping part of phase space and assuming that π^0 flow value is the same as that for charged particles (which are predominately charged pions). The results are shown in Fig. 7 for both the PMD data and the simulation using input π^0 anisotropy. The photon anisotropy coefficients extracted from the simulated PMD data are consistent within errors with the measured PMD results.

The use of PMD data to determine the event plane gives a strong π^0 decay effect. This is shown by open circles in Fig. 7 which show simulation results of anisotropy in PMD for isotropic π^0 emission. It is seen that the first order anisotropy coefficients are dominated by the decay effect. Although second order coefficients also have significant decay contribution, the measured values are much higher.

This is the first time that a fully consistent result is obtained both from charged particle anisotropy studies and photon anisotropy studies which are in agreement with each other.

3.3. Chiral symmetry restoration and disoriented chiral condensates

The restoration of chiral symmetry and its subsequent breaking through a phase transition has been predicted to create Disoriented Chiral Condensates (DCC) [23]. This phenomenon has been predicted to cause anomalous fluctuations in the relative production of charged and neutral pions in high energy hadronic and nuclear collisions in certain phase space regions (domains). It is predicted that the neutral pion fraction $f = \frac{N_{\pi^o}}{N_{\pi^o}+N_{\pi^\pm}}$ should follow a $1/\sqrt{f}$ distribution in the case of DCC formation in contrast to the binomial distribution for generic particle production. A number of methods has been proposed to study the formation of DCC (see references in [23]).

The formation of DCC has been studied extensively using the data from the two detectors, SPMD and PMD, measuring respectively the multiplicity of charged particles and photons in

overlapping part of phase space in the WA98 experiment.

3.3.1. Correlation and wavelet analysis : DCC has been studied in the WA98 experiment by various methods, both in the full overlapping phase space of the two detectors and also within smaller azimuthal domains [4, 6, 8]. Approaches based on direct correlation between charged particle and photon multiplicities event-by-event and discrete wavelet transform method have been used to study the distributions and their widths (rms values) looking for evidence of non-statistical fluctuation when compared with various mixed event formulations.

By constructing a set of mixed events to study various detector effects, the analysis showed that there exist non-statistical fluctuation individually in photon and charged particle production. However a correlated fluctuation has not been observed by this method of analysis. These results have been further compared with the predictions of a simple DCC model where DCC effect is introduced in the particle distribution of an event from a VENUS event generator at freezout by pairwise flipping of charged and neutral pions according to the $1/\sqrt{f}$ probability in a selected $(\eta-\phi)$ domain. The resulting distribution, after allowing π^0 to decay, is then analysed using the same correlation and wavelet analysis methods. An upper limit on the production of DCC-like fluctuation is estimated to be 10^{-2} for $\Delta\phi$ between 45-90° and 3×10^{-3} for $\Delta\phi$ between 90-135° for the top 5% centrality.

Further studies have also been carried out for the effect of centrality [8]. The upper limit curves are shown in Fig. 8 as a function of the azimuthal window for two centralities, top 5% (solid lines) and top 5-10% (dashed lines). It is observed that the fluctuations may be more at lower centralities.

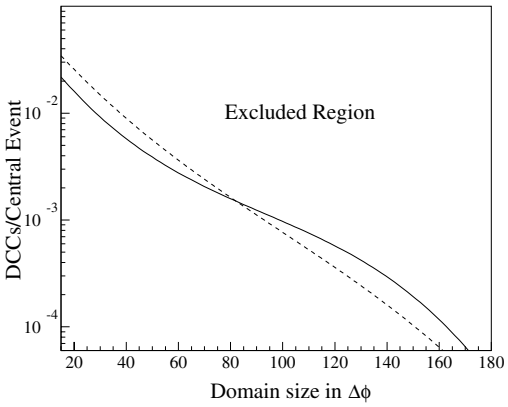

Figure 8. The 90% confidence level upper limit on DCC formation for central Pb+Pb collisions at 158A GeV, as a function of domain size in azimuthal angle within the context of a simple DCC model and the measured photon and charged particle multiplicities in the interval $2.9\leq \eta \leq 3.75$.

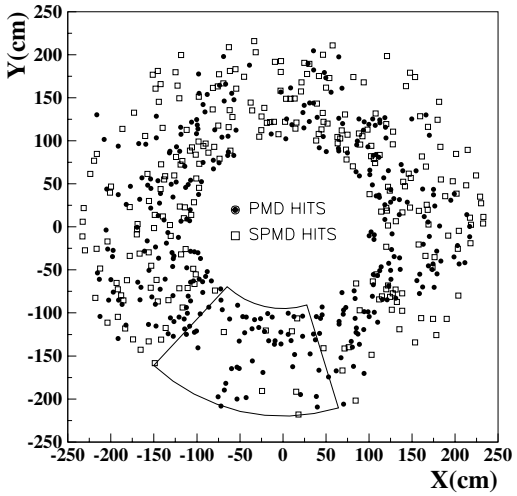

Figure 9. Plot showing photon hits (PMD) and charged particle hits (SPMD) in an azimuthal plane. The marked patch shows a region where number of charged particles are very less compared to photons.

3.3.2. Sliding window method : Several methods have been developed [24, 25] for the study of unusual structures in events arising due to non-statistical fluctuations resulting from phase

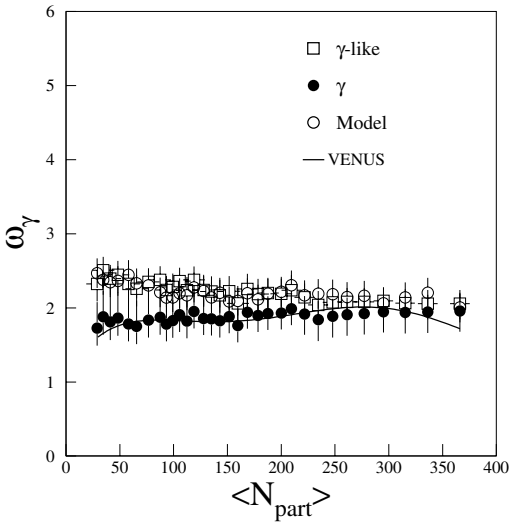

Figure 10. The relative fluctuations, ω_γ of photons as a function of number of participants. These are compared to calculations from a participant model and those from VENUS event generator.

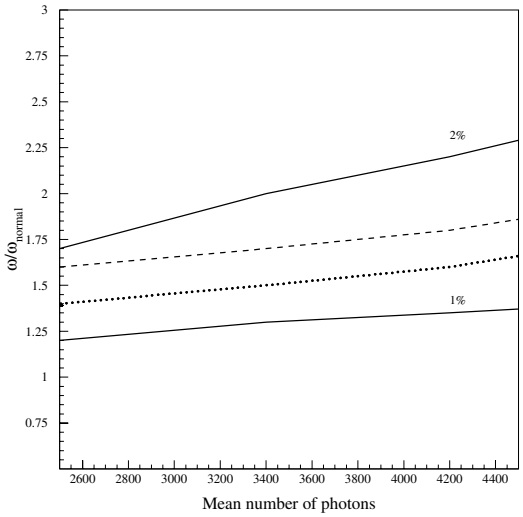

Figure 11. Fluctuation ω/ω_{normal} as a function of centrality. The dotted and dashed lines show the limits due to detector effects for a standalone PMD and for PMD with upstream material in the ALICE environment.

transitions. The sliding window method (SWM) is particularly appealing for the study of charge-neutral fluctuations and search for Centauro and anti-Centauro like events through model-independent direct observation. Some details of the method and preliminary results for the WA98 experiment are given in Ref. [25]. A typical event with an anti-Centauro like patch identified by the SWM is shown in Fig. 9, displaying PMD hits (filled circles) and SPMD hits (open boxes), projected onto the PMD plane, within the overlapping (η, ϕ) zone. The marked 60° patch corresponds to $f = 0.8$, this has only 7 charged particle hits as compared to 55 photon hits.

The percentage of events having exotic patches in data, with f-values beyond 4.5σ of the generic f- distribution, is found to be 0.39 ± 0.016, as compared to 0.081 ± 0.007 in mixed events and 0.013 ± 0.008 in GEANT simulated VENUS events. These patches are almost uniformly distributed in azimuth. Although a direct comparison with the results of upper limits, described in the previous section is not possible, the present value of 0.39% seems within the expected range. The present results are based on direct observation of event structure and are model-independent. The results, however, are preliminary and further checks are in progress to study the detector related effects as this is an important observation.

3.4. Multiplicity fluctuation

With the production of large number of particles on an event-by-event basis in high energy heavy ion collisions, it is very important to study anomalous fluctuations of multiplicity which is a major signal of QGP phase transition [26]. It has been proposed that event-by-event multiplicity fluctuations can arise from density fluctuations or droplet formation due to first order phase transition [27]. Large fluctuations in multiplicity are also expected at the tricritical point of QCD phase diagram [28]. Event-by-event fluctuations in the multiplicities of photons and charged particles have been studied in the WA98 experiment at CERN-SPS [7]. Fig. 10

shows the relative fluctuations, ω_γ $(= \sigma^2/N_\gamma)$ of photons as a function of mean number of participants. The data presented show the fluctuations in $\gamma - like$ clusters (open squares) and photons after correction for efficiency and purity (filled circles).

These are compared to calculations from a participant model [29] and those from VENUS event generator. The centrality dependence of charged particle multiplicity fluctuation in the measured data is found to agree reasonably well with those obtained from the participant model. However, for photons the multiplicity fluctuation has been found to be lower compared to those obtained from the participant model.

4. Future possibilities

The study of anisotropy of produced particles will remain a major goal of the PMD. One can deduce the flow values for neutral pions and compare with those for charged pions measured using other subsystems. The PMD will also provide the event plane information for the study of anisotropic emission of particles in any other rapidity window, both in STAR and in ALICE experiments. The usefulness of PMD has already been studied in the context of anisotropic emission of J/Ψ particles in the ALICE dimuon spcetroemter [30].

The STAR experiment has a forward time projection chamber (FTPC) in a pseudorapidity region which is overlapping with the coverage of the PMD. The FTPC provides a measure of charged particle multiplicity as well as their momenta. Using the momentum selection of charged particles, the study of DCC-like charged neutral fluctuation should be possible with improved results as has been shown by simulation studies [31]. It is shown that the p_T selection of charged particles enhances the DCC signal considerably more than that of photons.

In the ALICE experiment at the LHC, the much higher multiplicity of produced particles should result in highly reduced statistical fluctuation and consequently enhanced sensitivity to dynamical fluctuation. Possible physics studies with the PMD in ALICE have been presented in Refs. [13, 16]. The forward multiplicity detector (FMD) in ALICE has the (η, ϕ) coverage overlapping with those of the PMD. The FMD-PMD pair is expected to be used for the study of charged-neutral fluctuation at the LHC energy.

The sensitivity of the PMD to small fluctuations has been studied using the fluctuation measure $\omega = \sigma^2_\gamma/N_\gamma$ in a fast simulation technique where dynamical fluctuation has been introduced in the particle distribution to make it wider. The resulting distribution is again analyzed for the same fluctuation measure. Fig. 11 shows the ratio of fluctuation measure after and before introducing the dynamical component plotted as a function of the mean multiplicity of photons in PMD. It is found that dynamical fluctuation as low as 2% can be observed with the PMD even at lower multiplicities. As the statistical fluctuation decreases with increasing multiplicity, the difference between the limits set by detector effects and the dynamical fluctuation increases, providing more sensitivity at higher multiplicity.

5. Summary

Using a fine granularity preshower photon multiplicity detector (PMD), important contribution has ben made to the study of ultra-relativistic heavy ion collisions. Beginning with a detector made of plastic scintillator pads and wavelength shifting optical fibres for the SPS experiments, the PMD for the RHIC and LHC colliders has been made in the form of honeycomb gas proportional counters using a novel concept of extended cathode. Among the important studies at the SPS are first observation of collective flow and a detailed study of localized charged-neutral fluctuation as a probe for DCC. In addition the PMD's contribution include study of pseudo-rapidity distributions of photons, scaling of photon multiplicity with number of participating nucleons, centrality dependence of $< p_T >$ of photons and event-by-event fluctuations in photon multiplicity. The PMD is taking data at the RHIC collider and is expected to be installed in ALICE experiment at the LHC in 2007. The RHIC program has already paid dividends in the

study of limiting fragmentation of identified particles. The study of DCC will be continued at the RHIC using the PMD and the FTPC in STAR experiment and at the LHC using the PMD and the FMD in the ALICE experiment. At the LHC, larger multiplicity will be helpful in studying the event-by-event fluctuation in global observables with better precision.

Acknowledgments

The experimental program for the study of quark-gluon plasma at CERN and BNL is funded by the Department of Atomic Energy and the Department of Science and Technology of the Government of India. In addition the program has also derived financial support from the University Grants Commission and the Council of Scientific and Industrial Research of the Government of India, the STAR Collaboration, the CERN NMS grants, and the Indo-German Exchange Program in various stages of the work. We acknowledge the collaborative work of all the team members, past and present, of the WA93 collaboration, WA98 collaboration, STAR collaboration and ALICE Collaboration. We acknowledge the extensive support received from the engineering and technical manpower and computer facility personnel at BNL and CERN and also at all the collaborating institutions, namely VECC Kolkata, IOP Bhubaneswar, Panjab University Chandigarh, University of Rajasthan Jaipur, University of Jammu, Jammu and GSI Darmstadt.

References

[1] Aggarwal M.M. et al, WA93 Collaboration, 1997, *Phys. Lett.* **B403** 207.
[2] Aggarwal M.M. et al, WA93 Collaboration, 1997, *Phys. Lett.* **B404** 207.
[3] Aggarwal M.M. et al, WA93 Collaboration, 1998, *Phys. Rev.* **C58** 1146.
[4] Aggarwal M.M. et al, WA98 Collaboration, 1998, *Phys. Lett.* **B420** 169.
[5] Aggarwal M.M. et al, WA98 Collaboration, 1999, *Phys. Lett.* **B458** 422.
[6] Aggarwal M.M. et al, WA98 Collaboration, 2001, *Phys. Rev.* **C64** 011901.
[7] Aggarwal M.M. *et al.*, WA98 Collaboration, 2002, *Phys. Rev.* **C 65** 054912.
[8] Aggarwal M.M. et al, WA98 Collaboration, 2003, *Phys. Rev.* **C67** 044901.
[9] Aggarwal M.M. *et al.*, WA98 Collaboration, 2005, *Eur. Phys. J* **C41** 287.
[10] Adams J. *et al.*, STAR Collaboration, 2005, *Phys. Rev. Lett.* **95** 062301.
[11] Aggarwal M.M. et al., 1996, *Nucl. Instr. Meth.* **A372** 143.
[12] Aggarwal M.M. et al., 1999, *Nucl. Instr. Meth.* **A424** 395.
[13] ALICE Technical Design Report on Photon Multiplicity Detector ,1999, CERN/LHCC 99-32.
[14] Aggarwal M.M. et al., 2002, *Nucl. Instr. Meth.* **A488** 131.
[15] Aggarwal M.M. et al., 2003, *Nucl. Instr. Meth.* **A499** 751.
[16] ALICE Technical Design Report on Photon Multiplicity Detector, Addendum-1, CERN/LHCC 2003-038 (2003).
[17] Carminati F. et al., Physics Performance Report of ALICE Vol. I, 2004, *Jour. Phys. G, Nucl. Part. Phys.* **30** 1654.
[18] Chattopadhyay S., Ahammed Z. and Viyogi Y.P., 1999, *Nucl. Instrum. Meth.* **A421** 558.
[19] Werner K., 1993 *Phys. Rep.* **C232** 87.
[20] Mohanty B. et al, STAR Collaboration, contribution in these proceedings.
[21] Ollitrault J.-Y., 1992, *Phys. Rev.* **D46** 229.
[22] Raniwala R., Raniwala S., Viyogi Y.P., 2000, *Phys. Lett.* **B489** 9.
[23] Mohanty B. and Serreau B., 2005, *Phys. Rept.* **414** 263 and references therein.
[24] Das A.C. and Viyogi Y.P., 1996, *Phys.Lett.* **B380** 437; Aggarwal M.M., Bhatia V.S., Das A.C. and Viyogi Y.P., 1998, *Phys.Lett.* **B438** 357.
[25] Aggarwal M.M.,WA98 Collaboration, 2003, *Pramana* **60** 987.
[26] Heiselberg H., 2001, *Phys. Rep.* **351** 161.
[27] Van Hove L., 1984, *Z. Phys.* **C 21** 93; Kapusta J.I., Vischer A.P., 1995, *Phys. Rev.* **C 52** 2725.
[28] Stephanov M., Rajagopal K. and Shuryak E., 1998, *Phys. Rev. Lett.* **81** 4816.
[29] Baym G. and Heiselberg H., 1999, *Phys. Lett.* **B469** 7; Baym G. et al., *Phys. Lett.* **B219** 205.
[30] Morsch A., Raniwala R., Raniwala S., Viyogi Y.P., 2001, ALICE Internal Note ALICE-INT-2001-22.
[31] Mohanty B., Nayak T.K., Mahapatra D.P. and Viyogi Y.P., 2004, *Int. J. Mod. Phys.* **A19** 1453.